In situ FTIR and UV/VIS spectroscopic study of the generation of anionic Pt–carbonyl complexes within a faujasite matrix

G. Schulz-Ekloff, R.J. Lipski, N.I. Jaeger, P. Hülstede

Institut für Angewandte und Physikalische Chemie, Universität Bremen – FB 2, PF 330 440, 28334 Bremen, Germany

and

L. Kubelkova

J. Heyrovsky Institute of Physical Chemistry and Electrochemistry, Czech Academy of Sciences, Dolejskova 3, 18233 Prague 8, Czech Republic

Received 18 July 1994; accepted 26 October 1994

The temporal generation of anionic platinum–carbonyl complexes in platinum ion-exchanged zeolites X and Y by reductive carbonylation at 10^5 Pa and 363 K is monitored by in situ UV/VIS and FTIR spectroscopy. A monomer $[Pt_3(CO)_6]^{2-}$, exhibiting bands at 318 and 456 nm in the UV/VIS spectra and at 1790 and 2025 cm^{-1} in the FTIR spectra, is the only platinum/species formed in NaX. The monomer as well as oligomers are generated in NaY, where the formation of the latter species is due to the stronger acidity in the NaY as compared to NaX. The decomposition of the complexes results in the generation of Pt clusters of the size $\leqslant 1$ nm.

Keywords: anionic Pt–carbonyl complexes; CO chemisorption on Pt; IR spectroscopy; UV/VIS diffuse reflectance spectroscopy; faujasites

1. Introduction

The investigation of structure–function relationships in the case of supported metal catalysts requires the preparation of well-defined metal dispersions with variable and narrow particle size distributions.

Recent progress in the preparation of tailor-made metal dispersions has been achieved, e.g., by Schubert et al. [1,2] via the sol–gel synthesis route, or for monodispersed supported metal clusters in the interesting size range $\leqslant 1$ nm by Schmid et al. [3] from cluster compounds, or within a faujasite by Sachtler et al. [4].

Zeolites are known to be a suitable matrix for the preparation of metal disper-

© J.C. Baltzer AG, Science Publishers

sions with variable and narrow particle size distributions [5,6] and for the heterogenization of homogeneous catalysts by a ship-in-the-bottle synthesis [7–9]. This approach has recently been extended to the synthesis of anionic Pt–carbonyl complexes within the supercages of a faujasite by de Mallmann and Barthomeuf [10] and by Li et al. [11]. The platinum–carbonyl dianions of the general formula $[Pt_3(CO)_6]_n^{2-}$ consist of a chain of $Pt_3(CO)_6$ units in a so-called tinker toy construction [12]. Dianionic carbonyl complexes of catalytically active metals have been prepared and characterized first in homogeneous phase by Calabrese et al. [13] and by Longoni and Chini [14].

The mechanism of the formation and the aggregation of the complexes within the supercages of faujasites is still under discussion. In the following study the dynamics of the ship-in-the-bottle synthesis of Pt–carbonyl dianions inside faujasite matrices of different basicity will be followed and the resulting complexes will be characterized by in situ FTIR and UV/VIS spectroscopy. Via decomposition of the complexes under mild conditions the formation of small Pt cluster can be achieved.

2. Experimental

2.1. SAMPLE PREPARATION

Faujasites NaX (Si/Al = 1.18) and NaY (Si/Al = 2.76) were loaded with 4 wt% Pt by ion exchange with the appropriate amount of the platinum tetraammine complex and dried at 360 K. The samples are designated PtNaX and PtNaY.

Reductive carbonylation was carried out following the evacuation of the samples at 360 K for 5 h. Starting at 298 K, the platinum loaded zeolites were heated under a static pressure of 10^5 Pa CO to 363 K (1–2 K/min) and the progressing formation of the Pt–carbonyl dianions followed by in situ spectroscopy over a period of up to 96 h.

The crystallinity of the samples was checked by X-ray diffraction and by N_2-physisorption at all stages of the experiment and no loss could be detected.

2.2. FTIR AND UV/VIS SPECTROSCOPY

Formation and decomposition of the complex could be observed by in situ FTIR and UV/VIS spectroscopy. FTIR spectra were recorded between 2100 and 1700 cm^{-1} on a Biorad FTS 60A spectrometer with a resolution of 2 cm^{-1} and an accumulation of 80 scans requiring a recording time of 1 min. The thin sample wafers (5–6 mg/cm^2) were mounted in a gold grid to achieve mechanical stability and optimal contact of the wafers to the sample holder. Temperature gradients across the specimen could thus be minimized [15].

UV/VIS spectra were recorded on a Cary 4 spectrophotometer in diffuse reflec-

tance with a praying mantis. Wafers of the Pt-loaded NaY and NaX material (thickness 1 mm, diameter 5 mm, weight 20 mg) were placed in an evacuable chamber (Fa. Harrick) on a gold grid sample holder in order to minimize temperature gradients across the specimen. The spectra were recorded in a range between 200 and 800 nm. The distance between measuring points was 1 nm and the integration time 0.5 s corresponding to a scan speed of 120 nm/min. All spectra were recorded with a spectral band width of 4 nm.

The wafer can be regarded as infinitely thick as required by the Kubelka–Munk theory. Samples were diluted with unloaded zeolite in order to provide a weakly absorbing specimen with the Kubelka–Munk function proportional to the concentration of the absorbing species.

The Kubelka–Munk function was calculated according to

$$F(R_\infty) = \frac{(1 - R_\infty)^2}{2R_\infty} = \frac{k}{s}$$

with R_∞ the absolute reflectivity, k the absorption coefficient and s the scattering coefficient.

To obtain the absolute reflectivity, the spectrum of a standard with a known reflectivity (Fa. LOT) is used as a reference spectrum:

$$R_{\text{sample},\infty} = \frac{R_{\text{sample,chamber}}}{R_{\text{mixture,chamber}}} \frac{R_{\text{mixture}}}{R_{\text{standard}}},$$

where R_{mixture} is the reflectivity of the sample mixture (zeolite + Pt-loaded zeolite) at ambient conditions, measured with a praying mantis. R_{standard} is the reflectivity of the standard measured at the same conditions as R_{mixture}. $R_{\text{mixture,chamber}}$ is the reflectivity of a wafer of the sample mixture measured in a reaction chamber in the praying mantis prior to the reaction. $R_{\text{sample,chamber}}$ is the reflectivity of the sample wafer in the reaction chamber during the reaction. The form of this equation is due to the impossibility of measuring the standard in the reaction chamber. So spectra of the sample mixture have to be recorded in the praying mantis without the chamber and then this relative reflectivity can be used as a base spectrum.

The absorption of the sample mixture before the reaction is eliminated by subtracting the Kubelka–Munk function of the mixture from that of the sample:

$$F(R_\infty) = F(R_{\text{sample},\infty}) - F\left(\frac{R_{\text{mixture}}}{R_{\text{standard}}}\right).$$

The $F(R_\infty)$ values should only contain the absorption by the platinum and its interaction with CO.

3. Results

The evolution of the Pt–carbonyl complexes as observed by in situ FTIR and UV/VIS spectroscopy is depicted in figs. 1 and 2 for PtNaX and in figs. 3 and 4 for

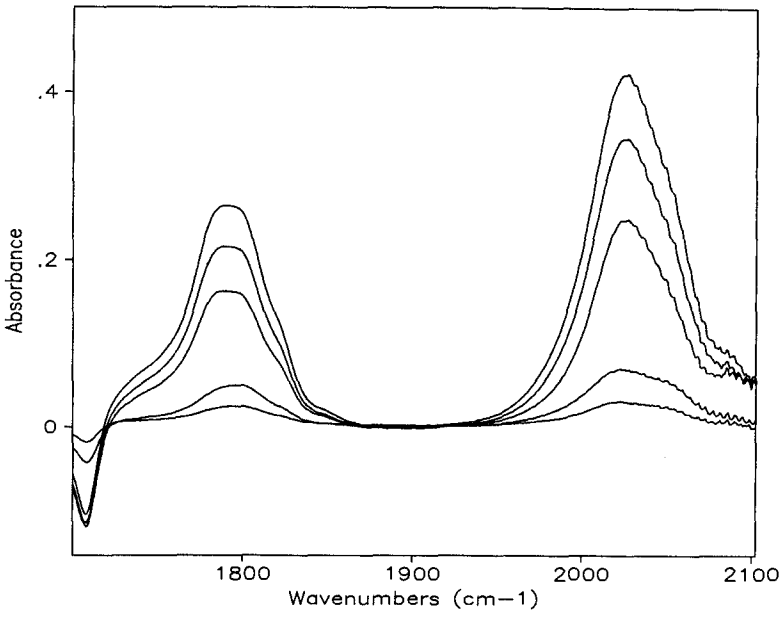

Fig. 1. Reductive carbonylation of PtNaX (10^5 Pa CO, 363 K). FTIR spectra were recorded after 6, 10, 24.5 and 30.5 h reaction time. The evolution of the maxima at 1790 and 2025 cm^{-1} represents the formation of the $[Pt_3(CO)_6]^{2-}$ monomer.

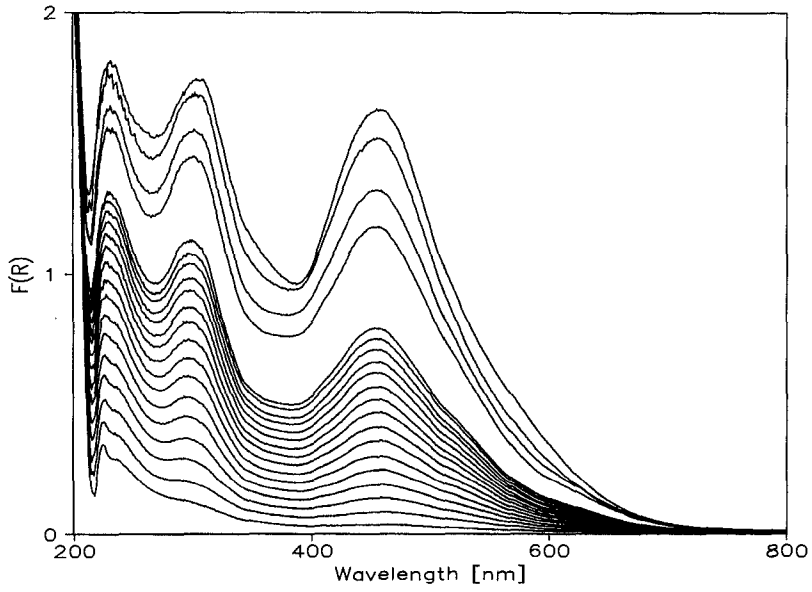

Fig. 2. Reductive carbonylation of PtNaX (10^5 Pa CO, 363 K). The UV/VIS spectra were recorded every 15 min during the first 4 h of the reaction (lower part of the figure) thereafter at 8, 24 and 48 h (upper three curves). The information contained in the peaks at 318 nm and 456 nm is complementary to the FTIR spectra.

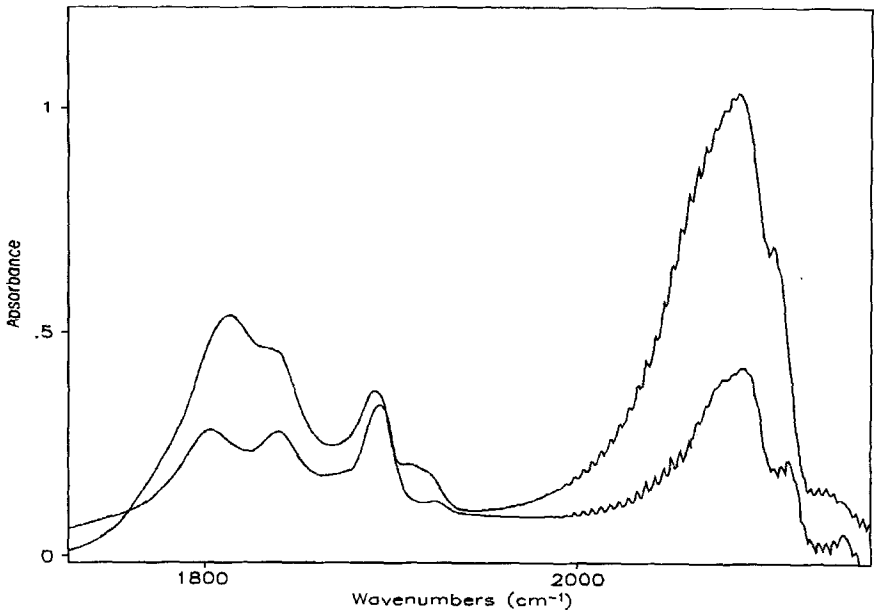

Fig. 3. Reductive carbonylation of PtNaY (10^5 Pa CO, 363 K). Two FTIR spectra recorded after 8 h and 35.5 h reaction time are depicted. The evolution of maxima at 1840, 1895 and 1920 cm^{-1} is due to the formation of a $[Pt_3(CO)_6]_n^{2-}$ ($n \geqslant 3$) complex via oligomerization of the $[Pt_3(CO)_6]^{2-}$ monomer (1815, 2088 cm^{-1}).

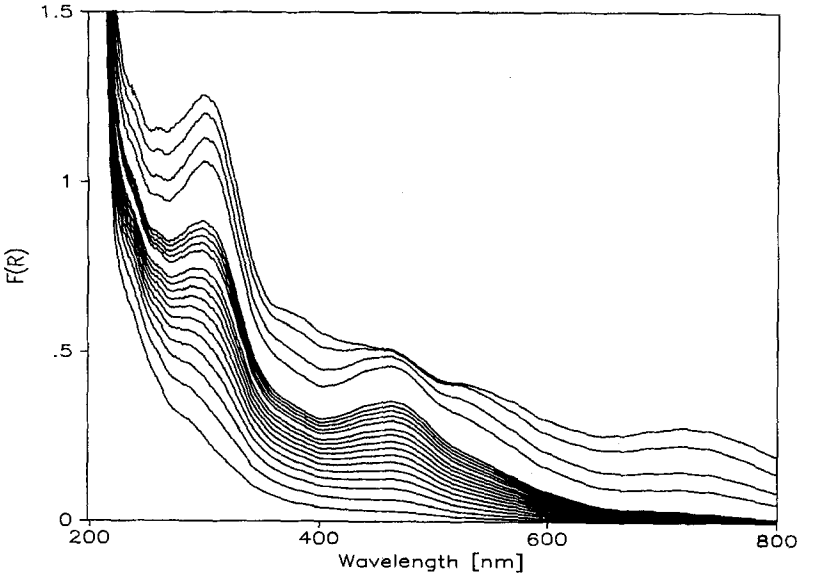

Fig. 4. Reductive carbonylation of PtNaY (10^5 Pa CO, 363 K). The UV/VIS spectra were recorded every 15 min during the first 4 h of the reaction (lower part of the figure), thereafter at 8, 24, 48, 72 and 96 h reaction time (upper 5 curves). The information contained in the peaks at 312, 384, 457, 512 and 725 nm is complementary to the FTIR spectra.

PtNaY, respectively. The complexes are formed in a slow process which under the given experimental conditions is completed after several days. The positions of the main absorption peaks in the final spectra and their assignment are summarized in table 1.

In the case of NaX the FTIR spectra (fig. 1) as well as the UV/VIS spectra (fig. 2) show the evolution of two clearly distinguishable peaks. Fig. 1 shows FTIR spectra recorded after reaction times of 6, 10, 24.5, 30.5 and 34.5 h with two peaks at 1790 and 2025 cm^{-1}. In addition, a decreasing band at 1710 cm^{-1} can be clearly observed in fig. 1. The UV/VIS spectra were recorded every 15 min during the first 4 h reaction time (lower part of fig. 2) and after 8, 24 and 48 h (upper three spectra in fig. 2) after which time the reaction apparently was completed. The position of the two peaks at 318 and 456 nm remained unchanged during the reaction. In addition a weak shoulder is present on the red flank of the 456 nm peak (fig. 2). The specimen shows an orange-brown colour.

In the case of PtNaY the spectra depicted in figs. 3 and 4 show a more complex structure. Fig. 3 shows two FTIR spectra recorded after 8 and 35.5 h reaction time. After that time no noticeable changes in peak position and absorbance could be observed. The final spectrum exhibits five clearly distinguishable peaks at 1815, 1840, 1895, 1920 and 2088 cm^{-1}. The corresponding evolution of the UV/VIS spectra is shown in fig. 4. During the first 4 h spectra were recorded every 15 min (lower part of fig. 4) and the growth of only two absorption bands at 312 and 457 nm can be clearly recognized. Three more bands at 384, 512 and 725 nm evolve thereafter, as can be seen in the successive spectra recorded after 8, 24, 48, 72 and 96 h reaction time. Thereafter no further changes in $F(R)$ could be observed.

In the UV/VIS spectra of PtNaX (fig. 2) an additional peak is found at 230 nm and the spectra of PtNaY show a small shoulder at the same wavelength (fig. 4).

The thermal decomposition of the carbonyls was achieved by raising the temperature to 423 K while maintaining the static pressure of CO (10^5 Pa). The structure of the UV/VIS spectrum disappeared within 2 h and the Kubelka–Munk function upon evacuation of the sample showed a constant value between 300 and

Table 1
Position of main absorption peaks in the final FTIR and UV/VIS spectra and assignment to the size n of the dianionic Pt–carbonyl complex $[Pt_3(CO)_6]_n^{2-}$

Sample	FTIR spectrum (cm^{-1})	UV/VIS spectrum (nm)	n
PtNaX	1790	318	1
	2025	456	1
PtNaY	1815	312	1
	2088	457	1
	1840	384	3–4
	2108 (sh)	512	3–4
	1895, 1920	725	$\geqslant 5$

800 nm. Exposure of the sample to CO (10^4 Pa, 298 K) led to a spectrum with maxima at 1800 and 2080 cm^{-1} (fig. 5).

4. Discussion

The formation of the anionic platinum–carbonyl complex proceeds via reductive carbonylation of the $[Pt(NH_3)_4]^{2+}$ complex present in the ion-exchanged samples. The evolution of the dominant bands in both the FTIR and the UV/VIS spectra occurs in parallel and on the same time scale. It is therefore concluded that the same species are observed in both spectroscopies. The first step of this reaction can be summarized by the equation, which implicitly contains the LTWGS reaction,

$$3nPt^{2+} + (9n+1)CO + (3n+1)H_2O \rightarrow [Pt_3(CO)_6]_n^{2-} + (3n+1)CO_2 + 2(3n+1)H^+ .$$

(1) The reduction requires hydrogen which is produced via the low temperature water–gas shift reaction (LTWGS) [16]. (2) This means that the complexes cannot be formed in the absence of water. (3) The water present in the samples following the evacuation at 360 K for 5 h proved to be sufficient for the reaction to proceed.

Fig. 5. Adsorption of CO on PtNaY (10^4 Pa CO, 298 K followed by evacuation) following the decomposition of the anionic carbonyl complexes under mild conditions (10^{-2} Pa CO, 423 K). The maxima in the spectrum can be assigned to CO bridge-bonded (1800 cm^{-1}) and linearly bonded (2070 cm^{-1}) to small Pt particles.

The complexes $Pt_3(CO)_6]_n^{2-}$ of lateral dimension 0.9 nm [11] can be easily accommodated by the supercages of the faujasite up to $n = 3$ (inter Pt ring distance = 0.3 nm). Complexes of larger size can grow into adjacent supercages.

The combined analysis of the vibrational and the electronic spectra with reference to literature data allows a very satisfactory identification of the $[Pt_3(CO)_6]^{2-}$ monomer, which evolves predominantly in the case of the PtNaX sample (figs. 1 and 2). The size n of anionic carbonyl complexes and the position of the two UV/VIS absorption maxima in THF have been correlated by Chang et al. [17] as well as Bhaduri and Sharma [18,19] for $n \geqslant 3$. A linear extrapolation of the data of these authors (table 2) leads to the assignment of the bands at 318 and 456 nm (fig. 2) to the monomer $[Pt_3(CO)_6]^{2-}$, which is nearly exclusively formed in the case of PtNaX. The shoulder observed on the red flank of the 456 nm band (fig. 2) points to the formation of some oligomer with $n > 1$.

The UV/VIS absorption maxima observed for PtNaY (fig. 4) can be assigned to different species. The monomer can be identified by the peaks at 312 and 457 nm which are almost identical to the spectrum observed in fig. 2 for PtNaX. Oligomerization is indicated by the additional peaks. The maxima at 384 and 512 nm can be assigned to an oligomer with $n = 3$ or 4. The band at 725 nm belongs to a species with $n \geqslant 5$. The justification of this tentative assignment is again based upon the comparison with values reported in the literature for complexes dissolved in THF (table 2). No deconvolution of the spectra has been attempted. A possible interaction between the electronic states of the complex and the zeolite matrix, e.g. via distortion of the symmetry, cannot be accounted for at the present time. The interaction would be of the same nature in both samples. The process of oligomerization can be summarized as follows [11]:

$$2[Pt_3(CO)_6]^{2-} + 2H^+ \rightarrow [Pt_3(CO)_6]_2^{2-} + H_2 .$$

The more acidic nature of the NaY zeolite is in favour of the oligomerization reaction.

The peaks at 1790 and 2025 cm^{-1} observed in the FTIR spectra (fig. 1) can be assigned to bridge-bonded and terminal CO in the complex, respectively. The relationship between the size n of the metal complex and the absorption frequencies of the terminal and the bridge-bonded CO group has been reported by Longoni and Chini for the complex in THF solution [14]. In both cases a parallel shift of the fre-

Table 2
UV/VIS absorption maxima of anionic Pt–carbonyl complexes $[Pt_3(CO)_6]_n^{2-}$ in THF and size n

Wavelength (nm)	Size of cluster n	Ref.
410, 700	5	[17,22]
392, 620	4	[18]
370, 565	3	[18]
318, 456	1	this work

quencies to higher wave numbers with increasing n up to about $n = 6$ has been observed. For $n = 1$ a value of 1740 cm^{-1} for bridged and of 1945 cm^{-1} for terminal CO has been reported. For a supporting zeolite NaY matrix a shift of this value to a higher wave number by about 26–40 cm^{-1} [20] is expected. This can be related to the decrease in basicity with increasing Si/Al ratio [21]. In the case of the sample PtNaX a shift to higher wavenumbers as compared to the THF-dissolved complex could be observed for the bridge-bonded ($\Delta\nu = 50$ cm^{-1}) as well as for the terminal-bonded CO ($\Delta\nu = 80$ cm^{-1}) in contrast to a report [20] that the frequency for bridge-bonded CO is shifted into the opposite direction. This shift for zeolite-encaged complexes points to an attachment of protons resulting in a decrease of the donor properties of the Pt clusters to the CO ligands.

The interaction with the NaY matrix is expected to shift the frequency of the terminal CO group of the monomer to even higher wave numbers (2088 cm^{-1}, fig. 3), since the basicity is even lower than in NaX [20]. The pair of peaks at 1815 and 2088 cm^{-1} can be assigned to the monomer $[Pt_3(CO)_6]^{2-}$, which can be unambiguously identified in the UV/VIS spectrum (fig. 4). The identification of the monomer $[Pt_3(CO)_6]^{2-}$ in the UV/VIS spectrum opens the opportunity to quantify the influence of the zeolite matrix upon the shift of the C–O vibration frequency.

The assignment of the remaining peaks is less straightforward since bands belonging to the terminal CO group and corresponding to the clearly resolved peaks at 1895 and 1920 cm^{-1} (bridge-bonded CO) may be hidden under the broad maximum around 2088 cm^{-1}. The shoulder at 2108 cm^{-1} can be assigned to an oligomer with $n > 1$ since a shift to higher wavenumbers is expected for increasing n [14].

The band at 1710 cm^{-1} can be assigned to a formyl group [23] which may have formed in a side reaction in the course of the postulated water–gas shift reaction. Prior to the observed decrease of the absorbance with time an increase during the first 6 hours of the reaction could the observed (not shown in fig. 1).

The absorption at 230 nm in the UV/VIS spectra (figs. 2 and 4) can be attributed to small metallic Pt particles according to published experimental [24] and theoretical results [25]. Adsorption of CO on these particles might be hidden in the FTIR spectrum of the monomeric carbonyl complexes (fig. 1) and may be the reason for the shoulder observed on the high wavenumber flank of the absorption bands. This result indicates that the reduction of the Pt^{2+} to Pt(0) occurs in parallel to the formation of the carbonyls.

The decomposition of the complexes in specimen PtNaY under mild conditions followed by the adsorption of CO leads to an FTIR-spectrum which is characteristic of CO on very small ($\leqslant 1$ nm) Pt particles [15]. Both, the wavenumbers for linearly bonded CO (2070 cm^{-1}) and for bridge-bonded CO (1800 cm^{-1}) are shifted to lower wavenumbers compared to bulk Pt or larger Pt crystallites [16]. The metal particles could not be unambiguously identified by electron microscopy due to strong phase contrast of the intact zeolite matrix.

Formation of a monodispersed metal with a cluster size $\leqslant 1$ nm could thus be

achieved via decomposition of the anionic carbonyl complexes. It must be mentioned that the complexes can easily be decomposed in oxygen under ambient conditions. The procedure, however, results in a broad size distribution of large ($\geqslant 3-5$ nm) Pt crystallites predominantly located outside the zeolite host.

5. Conclusions

The spectra of anionic Pt–carbonyl complexes have been followed by in situ FTIR and UV/VIS spectroscopy. The spectra can be very satisfactorily assigned to the formation of a monomer $[Pt_3(CO)_6]^{2-}$ in the case of PtNaX. The observed oligomerization of the initially formed monomer in the case of PtNaY can be explained by the more acidic nature of this zeolite. This elucidates the mechanism which leads to the oligomers observed already by Barthomeuf [10] and by Li et al. [11] for NaY. The electronic spectra of the monomer served as a standard for the identification of this species also in PtNaY. As a consequence the even larger shift of the CO frequencies to higher wave numbers as compared to PtNaX could be correlated to the more acidic nature of NaY. Finally, the anionic Pt–carbonyl complexes can be used as suitable precursors for the formation of small Pt clusters within the zeolite host.

Acknowledgement

The authors are grateful to J. Klaas for providing the algorithm for calculating the Kubelka–Munk function. Financial support from the DFG (AZ 436 CSR 113-11) is gratefully acknowledged.

References

[1] B. Breitscheidel, J. Zieder and U. Schubert, Chem. Mater. 3 (1991) 559.
[2] U. Schubert, B. Breitscheidel, H. Buhler, Ch. Egger and W. Urbaniak, Mater. Res. Soc. Symp. Proc. 271 (1992) 621.
[3] G. Schmid, R. Kupper, H. Hess, J.-O. Mahn and J.-O. Bovin, Chem. Ber. 124 (1991) 1889.
[4] W.M.H. Sachtler and Z. Zhang, Adv. Catal. 39 (1993) 129.
[5] P. Gallezot, A. Alarcon-Diaz, J.-A. Dalmon, A.J. Renouprez and B.I. Imelik, J. Catal. 39 (1975) 334.
[6] A. Kleine, P.L. Ryder, N.I. Jaeger and G. Schulz-Ekloff, J. Chem. Soc. Faraday Trans. 82 (1986) 205.
[7] M. Ichikawa, Adv. Catal. 38 (1992) 283.
[8] G.A. Ozin and C. Gil, Chem. Rev. 89 (1989) 2831.
[9] G. Meyer, D. Wöhrle, M. Mohl and G. Schulz-Ekloff, J. Mol. Catal. 24 (1984) 115.
[10] A. de Mallmann and D. Barthomeuf, Catal. Lett. 5 (1990) 293.

[11] G.J. Li, T. Fujimoto, A. Fukuoka and M. Ichikawa, Catal. Lett. 12 (1992) 171.
[12] D.J. Underwood, R.H. Hoffmann, K. Tatsumi and Y. Yamamoto, J. Am. Chem. Soc. 107 (1985) 5968.
[13] J.C. Calabrese, L.F. Dahl, P. Chini and G. Longoni, J. Am. Chem. Soc. 96 (1974) 2614.
[14] G. Longoni and P. Chini, J. Am. Chem. Soc. 98 (1976) 7225.
[15] H. Bischoff, N.I. Jaeger and G. Schulz-Ekloff, Z. Phys. Chem. (Leipzig) 271 (1990) 1093.
[16] H. Bischoff, N.I. Jaeger, G. Schulz-Ekloff and L. Kubelkova, J. Mol. Catal. 80 (1993) 95.
[17] J.R. Chang, D.C. Koningsberger and B.C. Gates, J. Am. Chem. Soc. 114 (1992) 6460.
[18] S. Bhaduri and K.R. Sharma, J. Chem. Soc. Chem. Commun. (1983) 1412.
[19] S. Bhaduri and K.R. Sharma, J. Chem. Soc. Dalton Trans. (1984) 2309.
[20] G.J. Li, T. Fujimoto and M. Ichikawa, J. Chem. Soc. Chem. Commun. (1991) 1337.
[21] D. Barthomeuf, in: *Catalysis and Adsorption by Zeolites*, Studies in Surface Science and Catalysis, Vol. 65, eds. G. Öhlmann, H. Pfeifer and R. Fricke (Elsevier, Amsterdam, 1990) p. 157.
[22] A. Basu, S. Bhaduri and K.R. Sharma, J. Chem. Soc. Dalton Trans. (1984) 2315.
[23] A. Kiennemann, J.P. Hindermann, R. Breault and H. Idriss, ACS Symp. Ser. (1987) 328.
[24] T. Lopez, A. Romero and R. Gomez, J. Non-Cryst. Solids 127 (1991) 105.
[25] J.A. Creighton and D.G. Eadon, J. Chem. Soc. Faraday Trans. 87 (1991) 3881.